J|A|C|S COMMUNICATIONS

Published on Web 01/28/2010

Unexpected Facile Redistribution of Adsorbed Silica Nanoparticles Between Latexes

Jennifer A. Balmer,[†] Oleksandr O. Mykhaylyk,[†] J. Patrick A. Fairclough,[†] Anthony J. Ryan,[†] Steven P. Armes,*[,†] Martin W. Murray,[‡] Kenneth A. Murray,[‡] and Neal S. J. Williams[‡]

Dainton Building, Department of Chemistry, The University of Sheffield, Brook Hill, Sheffield, S3 7HF, United Kingdom, and AkzoNobel, Wexham Road, Slough, Berkshire, SL2 5DS, United Kingdom

Received December 1, 2009; E-mail: s.p.armes@sheffield.ac.uk

Colloidal nanocomposite particles are of considerable and growing interest to both academic and industrial scientists.[1−3] Potential applications for these nanocomposite particles include photonic devices,[4a] synthetic mimics for cosmic dust,[4b] and smart Pickering emulsifiers.[4c] One particularly successful commercial application is the use of film-forming nanocomposite particles in high performance exterior architectural coatings.[5] A common synthesis route involves *in situ* polymerization of a vinyl monomer in the presence of an ultrafine inorganic oxide sol (e.g. silica) to obtain colloidal nanocomposites with 'core−shell' morphologies via aqueous emulsion polymerization.[6,7] However, this approach can suffer from a relatively low silica aggregation efficiency. Moreover, excess silica sol can be detrimental to desirable properties such as film formation[8a] or emulsion stabilization[8b] and its removal is required for most characterization techniques. Fortunately, highly efficient colloidal nanocomposite formulations have been recently developed, which are desirable for commercial applications.[8a,c,d]

Recently we reported an alternative route for the preparation of 'core−shell' nanocomposites that involves physical adsorption of 20 nm silica particles onto a sterically stabilized poly(2-vinylpyridine) (P2VP)] latex in aqueous solution.[9] This approach allows facile variation of the P2VP latex core diameter and is easily extended to include other latexes; moreover, optimized protocols can produce a nanocomposite dispersion with no excess silica sol.

Herein we report an unprecedented and fascinating observation: addition of excess sterically stabilized P2VP latex to a colloidal dispersion of P2VP-silica nanocomposite particles (with silica shells at full monolayer coverage) leads to the facile redistribution of the silica nanoparticles such that *partial* coverage of all the P2VP latex particles is achieved (see Figure 1).

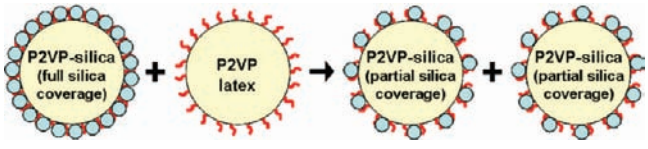

Figure 1. Schematic representation of the facile redistribution of silica nanoparticles upon addition of excess sterically stabilized P2VP latex to preformed P2VP-silica nanocomposite particles.

Three sterically stabilized P2VP latexes were prepared by cationic azo-initiated emulsion polymerization using a poly(ethylene glycol) monomethacrylate [PEGMA] macromonomer, as reported previously.[9,10] Latexes with approximate mean diameters of 300, 450, and 600 nm were readily obtained by judicious selection of the PEGMA stabilizer and Aliquat 336 surfactant concentrations and also by varying the total solids content for the polymerization (see Supporting Information for synthesis parameters [Table S1] and for latex diameters obtained by dynamic light scattering [DLS], small-angle x-ray scattering [SAXS], and transmission electron microscopy [TEM]). These three techniques confirmed that the P2VP latexes had spherical morphologies and relatively narrow size distributions. Preparation of 'core−shell' nanocomposite particles was achieved by simply mixing the aqueous P2VP latex and silica sol at 1.0 w/v % solids at a solution pH of 9−10. The silica sol concentration was chosen to ensure full monolayer coverage (i.e. $\theta = 1.00$) of the latex by the silica.[9] This protocol was used for all three P2VP latexes (see Figures 2 and S1). This 'heteroflocculation' route to colloidal nanocomposites[11] is based on a favorable interaction between the PEGMA stabilizer chains and the silica sol.[12] The adsorbed amounts (surface densities) of the PEGMA chains on the 450 and 600 nm P2VP latexes were determined to be 1.4 and 2.3 mg m^{-2}, as judged by ^{1}H NMR spectroscopy.[9] It is emphasized that nanocomposites are *not* formed on adding silica to an anionic charge-stabilized polystyrene latex (prepared using ammonium persulfate), presumably due to mutual electrostatic repulsion in this case (Figure S2).

In our initial experiments, 450 nm P2VP latex particles were added to preformed P2VP-silica nanocomposite particles such that

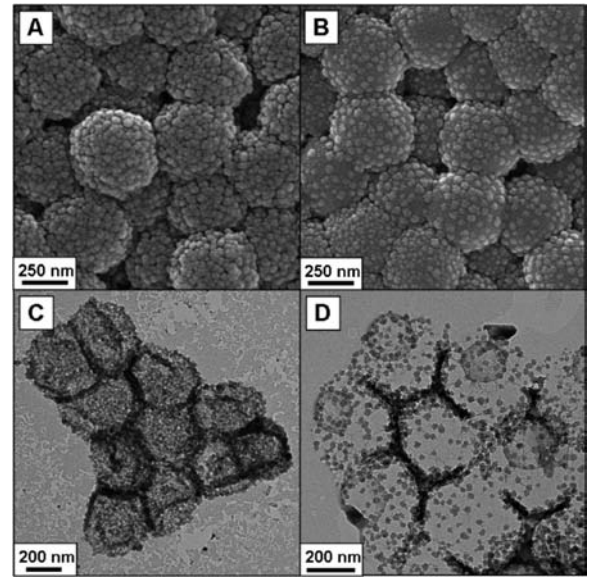

Figure 2. Electron micrographs obtained for: (a) P2VP-silica nanocomposite particles prepared by coating 450 nm P2VP latex with 20 nm silica [$\theta = 1.00$]; (b) P2VP-silica nanocomposite particles after addition of bare P2VP latex [$\theta = 0.33$]; (c) particles shown in (a) after calcination at 450 °C; (d) particles shown in (b) after calcination at 450 °C.

[†] University of Sheffield.
[‡] AkzoNobel.

10.1021/ja910139a

the nanocomposite/latex total surface area ratio was 1:2. Figure 2a shows a scanning electron microscopy (SEM) image of the P2VP-silica particles ($\theta = 1.00$) prior to the addition of any P2VP latex, while Figure 2b shows an image obtained after silica redistribution has occurred (for which $\theta = 0.33$). Close inspection confirms that, after addition of the P2VP latex, the silica coverage on the nanocomposite particles becomes distinctly patchy and the silica−silica separation distance increases significantly. Further evidence for silica exchange can be obtained from TEM images recorded after calcination of the particles at 450 °C; this thermal treatment causes pyrolysis of the P2VP latex component but leaves the silica intact. If the nanocomposite has a contiguous shell of silica particles ($\theta = 1.00$), hollow silica capsules can be obtained, whereas if the silica particles are present at submonolayer coverage ($\theta \ll 1$), a free-standing silica shell cannot be formed.[9] Figure 2c shows a TEM image of well-defined hollow silica capsules obtained after calcination of P2VP-silica nanocomposite particles for which $\theta = 1.00$. In contrast, Figure 2d shows the ill-defined silica morphology observed after calcination of P2VP-silica nanocomposite particles with submonolayer silica coverage ($\theta = 0.33$).

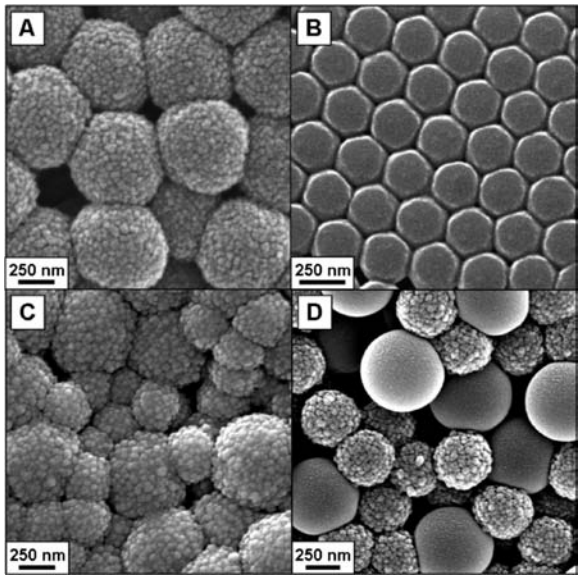

Figure 3. SEM images obtained for: (a) P2VP-silica nanocomposite particles prepared by coating a 600 nm sterically stabilized P2VP latex with 20 nm silica [such that the silica surface coverage $\theta = 1.00$]; (b) a 300 nm sterically stabilized P2VP latex; (c) a binary mixture of the P2VP-silica nanocomposite particles shown in (a) and the 300 nm P2VP latex [such that the final mean silica surface coverage $\theta = 0.50$]; (d) a binary mixture of a *charge-stabilized* anionic polystyrene latex added to P2VP-silica nanocomposite particles prepared by coating 450 nm P2VP latex with 20 nm silica (in this latter case no silica redistribution is observed).

Silica redistribution is also observed between different sized P2VP latexes. Thus, provided that both latexes have sufficiently narrow size distributions, this allows the latex diameter to be utilized as a convenient label. Figure 3a shows P2VP-silica nanocomposite particles prepared by coating the 600 nm latex with silica sol at full monolayer coverage ($\theta = 1.00$), while Figure 3b shows an image of an uncoated 300 nm P2VP latex. The binary dispersion shown in Figure 3c was obtained by mixing the P2VP-silica particles with the P2VP latex. Silica redistribution is again clearly evident: the silica particles now partially coat all the P2VP latex particles. Silica exchange is also observed when 600 nm P2VP latex is added to P2VP-silica nanocomposite particles prepared using the 300 nm P2VP latex (see Figure S3). In contrast, no silica redistribution occurs when anionic polystyrene latex is added to P2VP-silica nanocomposite particles. Instead, the latex and nanocomposite particles simply coexist as a binary mixture (see Figure 3d).

We have recently reported that 'core−shell' nanocomposite particles can also be prepared by *in situ* polymerization.[12,13] However, silica redistribution does *not* occur upon mixing latex with these *in situ* synthesized nanocomposite particles (see Figure S4). This suggests that, in this case, the silica particles are more strongly adsorbed onto (or partially embedded into) these latex cores than for the P2VP-silica nanocomposite particles prepared by heteroflocculation.

Although electron microscopy is very useful for characterizing nanocomposite particles, an integral technique such as SAXS is essential for obtaining robust nanostructural information in an aqueous solution. The relatively high electron density of silica compared to P2VP (see Supporting Information) provides good contrast and makes SAXS rather sensitive to the spatial location of the silica in the nanocomposite particles. The system shown in Figure 3a−3c was selected for SAXS analysis (see Figure 4). A step-by-step approach was used to obtain structural parameters for the nanocomposite particles from SAXS measurements (Figure 4c and 4e). First, the Irena SAS package[13] was used to fit the SAXS patterns obtained for the silica sol and P2VP latex alone (see Figure 4a and 4b respectively) and hence determine their weight-average diameters of 23 ± 6 nm and 573 ± 16 nm, respectively (see Table S2 for full details). These SAXS results are in agreement with particle diameters obtained from DLS measurements and electron microscopy images (Table S3). These structural parameters were then used to fit the SAXS pattern obtained for the P2VP-silica nanocomposite (Figure 4c), whose SEM image is presented in Figure 3a. A good fit to the data was obtained using a two-population model, which had been previously applied successfully to another core−shell system.[14] More specifically, a nanocomposite population with a 'core−shell' form factor was supplemented by a second population so as to account for the particulate nature of the silica shell surrounding the latex cores. The resulting structural parameters are summarized in Table S2. However, simply comparing the scattering patterns obtained for the P2VP latex (Figure 4b) and the corresponding P2VP-silica nanocomposite particles (Figure 4c) confirms that the minima (fringes) of the form factor shift toward lower q for the latter sample. This indicates that the overall particle diameter has increased upon addition of the silica sol, thus confirming the formation of core−shell nanocomposite particles in solution by heteroflocculation. This *in situ* observation is important, since it allows us to discount the possibility that the nanocomposite morphologies observed by electron microscopy are simply due to drying artifacts.

The SAXS pattern obtained for the partially coated nanocomposite particles after silica exchange between the large P2VP-silica nanocomposite particles (Figure 4c and 3a) and the small sterically stabilized P2VP latex (Figure 4d and 3b) for 1 h at 20 °C is shown in Figure 4e (see Figure 3c for the corresponding SEM image). If there had been no silica redistribution after mixing these two dispersions, this final scattering pattern would be simply the summation of the original latex and nanocomposite patterns (see Figure S6a in Supporting Information). This is clearly not the case. Instead, the observed SAXS curve is *a superposition of scattering patterns for two partially coated nanocomposite particles of different diameters* (see Figure S6b). This complex scattering pattern has been fitted using a three-population model comprising one population for the large nanocomposite core−shell particles, a second population for the small nanocomposite core−shell particles,

and a third population for the particulate silica shell that is present in both partially coated nanocomposites (see Table S2 for modeling parameters).

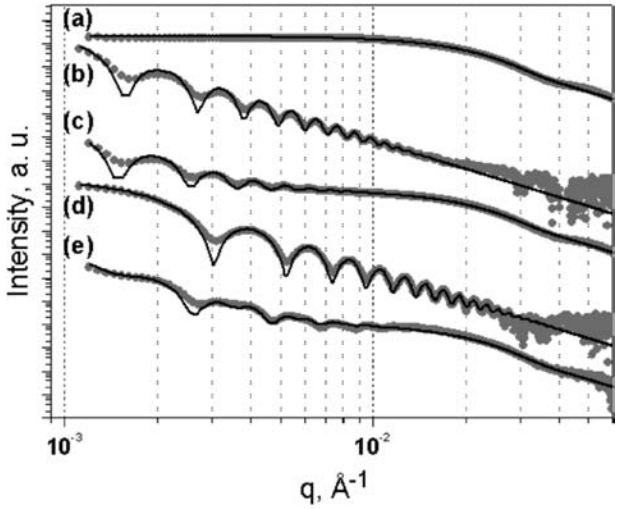

Figure 4. SAXS patterns and fits (solid lines) obtained for: (a) 20 nm silica sol; (b) 600 nm sterically stabilized P2VP latex; (c) P2VP-silica nanocomposite particles prepared by coating this 600 nm P2VP latex with 20 nm silica such that $\theta = 1.00$; (d) 300 nm sterically stabilized P2VP latex; (e) the final bimodal distribution of partially coated nanocomposite particles obtained after mixing dispersions (c) and (d) and allowing silica exchange to occur for 1 h at 20 °C. Each pattern has been multiplied by an arbitrary coefficient for clarity.

Thus our SAXS experiments confirm unambiguously that facile silica exchange occurs between nanocomposite and latex particles in aqueous solution. However, the present analysis does not provide any information regarding the kinetics of this redistribution process, other than that it appears to be complete within 1 h at 20 °C. Presumably, silica exchange between nanocomposite and latex particles occurs as a result of interparticle collisions caused by Brownian motion. Smoluchowski[15] showed that the half-life, $\tau_{1/2}$, of colloidal particles undergoing rapid coagulation in the absence of any repulsive forces (i.e., assuming 'sticky' interparticle collisions) is given by

$$\tau_{1/2} = 3\eta/4k_BTn_o$$

where η is the solution viscosity, k_B is Boltzmann's constant, T is the absolute temperature, and n_o is the particle concentration per unit volume. To a zeroth-order approximation, Smoluchowski's analysis should indicate a *lower limit* time scale for the kinetics of silica exchange. Under our experimental conditions ([P2VP-silica]$_o$ = [P2VP latex]$_o$ = 1.0 w/v %; 20 °C), we estimate a half-life of approximately 650 ms for silica exchange. We recently utilized time-resolved SAXS to study the kinetics of silica exchange using a stopped-flow cell at the European Synchrotron Radiation Facility (ESRF). Although not yet fully analyzed, our data are consistent with complete silica exchange occurring within time scales of a few seconds and will be reported in full elsewhere.

A versatile and rather generic commercial route to nanocomposite coatings involves mixing a film-forming latex with an ultrafine silica sol.[9,16] In some cases this approach is likely to involve physical adsorption of the silica onto the latex either prior to or during film formation. In view of our observations reported herein, it is interesting to consider to what extent the properties of the final dried nanocomposite coatings might be influenced by silica exchange occurring between latex particles (and possibly other paint components, such as pigment and filler particles) during film formation.

In summary, facile redistribution of adsorbed silica particles unexpectedly occurs on addition of excess sterically stabilized latex to core−shell polymer-silica nanocomposite particles. No silica exchange occurs if charge-stabilized anionic latexes are utilized, or if the nanocomposite particles are prepared via *in situ* polymerization rather than by heteroflocculation. These observations are expected to have important implications in the context of commercial nanocomposite formulations for the coatings industry, since control over the spatial distribution of the silica nanoparticles within the final nanocomposite film is vital for ensuring optimal transparency.

Acknowledgment. J.A.B. thanks AkzoNobel for an Industrial CASE EPSRC PhD studentship. S.P.A. is a recipient of a five-year Royal Society-Wolfson Research Merit Award. Eka Chemicals is thanked for donating the aqueous silica sol used in this work. The authors are grateful to ESRF for providing the beamtime and thank the personnel of ID02 station for their helpful assistance with the SAXS experiments. Jan Ilavsky is thanked for support with the Irena SAS package used for SAXS analysis.

Supporting Information Available: Full details of latex syntheses, SAXS experiments, and electron micrographs. This material is available free of charge via the Internet at http://pubs.acs.org.

References

(1) Balmer, J. A.; Schmid, A.; Armes, S. P. *J. Mater. Chem.* **2008**, *18*, 5722.
(2) Wang, T.; Keddie, J. L. *Adv. Colloid Interface Sci.* **2009**, *147*, 319.
(3) Zou, H.; Wu, S. S.; Shen, J. *Chem. Rev.* **2008**, *108*, 3893.
(4) (a) Mitzi, D. B. *Chem. Mater.* **2001**, *13*, 3283. (b) Burchell, M. J.; Willis, M. J.; Armes, S. P.; Khan, M. A.; Percy, M. J.; Perruchot, C. *Planet. Space Sci.* **2002**, *50*, 1025. (c) Fujii, S.; Read, E. S.; Binks, B. P.; Armes, S. P. *Adv. Mater.* **2005**, *17*, 1014.
(5) Tiarks, F.; Leuninger, J.; Wagner, O.; Jahns, E.; Wiese, H. *Surf. Coat. Int., Part A* **2007**, *90*, 221.
(6) Barthet, C.; Hickey, A. J.; Cairns, D. B.; Armes, S. P. *Adv. Mater.* **1999**, *11*, 408.
(7) Colver, P. J.; Colard, C. A. L.; Bon, S. A. F. *J. Am. Chem. Soc.* **2008**, *130*, 16850.
(8) (a) Schmid, A.; Scherl, P.; Armes, S. P.; Leite, C. A. P.; Galembeck, F. *Macromolecules* **2009**, *42*, 3721. (b) Fujii, S.; Armes, S. P.; Binks, B. P.; Murakami, R. *Langmuir* **2006**, *22*, 6818. (c) Dupin, D.; Schmid, A.; Balmer, J. A.; Armes, S. P. *Langmuir* **2007**, *23*, 11812. (d) Schmid, A.; Armes, S. P.; Leite, C. A. P.; Galembeck, F. *Langmuir* **2009**, *25*, 2486.
(9) Balmer, J. A.; Armes, S. P.; Fowler, P. W.; Tarnai, T.; Gáspár, Z.; Murray, K. A.; Williams, N. S. J. *Langmuir* **2009**, *25*, 5339.
(10) Dupin, D.; Fujii, S.; Armes, S. P.; Reeve, P.; Baxter, S. M. *Langmuir* **2006**, *22*, 3381.
(11) Harley, S.; Thompson, D. W.; Vincent, B. *Colloids Surf.* **1992**, *62*, 163.
(12) Cosgrove, T.; Griffiths, P. C.; Lloyd, P. M. *Langmuir* **1995**, *11*, 1457.
(13) Ilavsky, J.; Jemian, P. R. *J. Appl. Crystallogr.* **2009**, *42*, 347.
(14) Zhang, F.; Long, G. G.; Jemian, P. R.; Ilavsky, J.; Milam, V. T.; Lewis, J. A. *Langmuir* **2008**, *24*, 6504.
(15) Smoluchowski, M. *Phys. Z.* **1916**, *17*, 557–585.
(16) Greenwood, P.; Lagnemo, H. U.S. Patent No. 10683350, 2004.

JA910139A